

Learning Robust Anymodal Segmentor with Unimodal and Cross-modal Distillation

Xu Zheng¹ Haiwei Xue^{2,1} Jialei Chen³ Yibo Yan¹ Lutao Jiang¹ Yuanhuiyi Lyu¹ Kailun Yang⁴
Linfeng Zhang⁵ Xuming Hu¹

Abstract

Simultaneously using multimodal inputs from multiple sensors to train segmentors is intuitively advantageous but practically challenging. A key challenge is unimodal bias, where multimodal segmentors over-rely on certain modalities, causing performance drops when others are missing—common in real-world applications. To this end, we develop the **first** framework for learning robust segmentor that can handle any combinations of visual modalities. Specifically, we first introduce a parallel multimodal learning strategy for learning a strong teacher. The cross-modal and unimodal distillation is then achieved in the multiscale representation space by transferring the feature-level knowledge from multimodal to anymodal segmentors, aiming at addressing the unimodal bias and avoiding over-reliance on specific modalities. Moreover, a prediction-level modality-agnostic semantic distillation is proposed to achieve semantic knowledge transferring for segmentation. Extensive experiments on both synthetic and real-world multi-sensor benchmarks demonstrate that our method achieves superior performance (+6.37% & +6.15%).

1. Introduction

The success of multimodal deep learning relies heavily on effectively leveraging information from multiple modalities, particularly for complex tasks such as semantic segmentation in scene understanding. While intuitively beneficial, training segmentation models with inputs from multiple sensors presents significant practical challenges. A prominent issue in this context is **unimodal bias** — a phenomenon where networks develop an over-reliance on a single, faster-to-learn modality, often overlooking other sources of valu-

¹HKUST(GZ) ²Tsinghua University ³Nagoya University
⁴Hunan University ⁵Shanghai Jiao Tong University. Correspondence to: Xuming Hu <xuminghu@hkust-gz.edu.cn>.

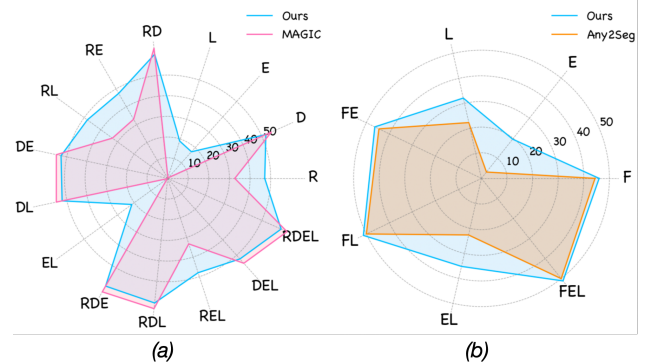


Figure 1. Comparison between ours against SoTA methods (Zheng et al., 2024b;a) on (a) MUSES and (b) DELIVER datasets.

able information. This bias stems from the distinct characteristics and varied learning dynamics of each sensor modality.

For example, the well-known CMX model (Zhang et al., 2023a) in multimodal semantic segmentation suffers significant performance drops when evaluated without the RGB modality. Meanwhile, the state-of-the-art model Any2Seg (Zheng et al., 2024a), which aims at learning modality-agnostic representation for missing modality problems, demonstrates a significant performance decline when evaluated in modality-incomplete scenarios. Specifically, when depth data is missing, segmentation performance drops markedly (RD: 68.21 \rightarrow R: 39.02, a decrease of 29.19 mIoU), illustrating how unimodal bias can lead to substantial performance degradation in real-world applications where certain modalities are often unavailable.

Despite advancements in multimodal learning, such as leveraging large multimodal language models (Zheng et al., 2024a) and prioritizing each modality (Zheng et al., 2024b), progress in addressing unimodal bias and fostering robust multimodal correlations remains limited. To address this gap, we introduce the first framework for learning robust anymodal segmentors¹. This framework is tailored to handle real-world scenarios where modality completeness cannot be guaranteed, such as missing modality (Liu et al., 2024) or modality-agnostic segmentation (Zheng et al., 2024a).

¹We define anymodal segmentors as models that ensure robust segmentation performance despite missing modalities.

Our approach begins with a novel **Parallel Multimodal Learning (PML)** strategy, which facilitates the learning of a strong teacher model for both unimodal and multimodal distillation without adding extra parameters. Inspired by recent methods (Zheng et al., 2024a;b), we process all multimodal inputs from different sensors in a single mini-batch, passing them through the segmentation model. Modality fusion is performed through simple averaging, and supervision is applied at the final layer of the segmentation decoder. This straightforward yet effective PML strategy enables segmentors to focus on capturing both unimodal and multimodal knowledge, as demonstrated in Tab. 5 and Tab. 6.

We then introduce a dual-level distillation process: Unimodal Distillation (UMD) and Cross-modal Distillation (CMD), applied across multi-scale representations and prediction levels. To simulate real-world scenarios, we apply an anymodal dropout strategy, where the multimodal inputs are randomly masked, creating varied modality combinations within each batch. For distribution distillation within the multi-scale representation space, the features from the anymodal segmentor are trained to align with the corresponding features from the multimodal teacher, thereby replicating the unimodal feature extraction capabilities. Furthermore, cross-modal correspondence is applied across all active modalities to mitigate the effects of unimodal bias. Finally, at the prediction level, we employ modality-agnostic semantic distillation to facilitate effective task-specific knowledge transfer between teacher and student models, further enhancing the robustness in diverse real-world conditions.

Extensive experiments on real-world and synthetic benchmarks demonstrate the superior robustness and performance of our method compared to existing state-of-the-art approaches, achieving mIoU improvements of +6.37% and +6.15%, respectively². Additionally, we analyze why fused multimodal fusion distillation is unsuitable for ensuring robustness in multimodal segmentation.

2. Related Work

2.1. Multimodal Semantic Segmentation

Semantic segmentation with multi-sensor inputs enhances scene understanding by leveraging complementary information from diverse sensors, such as event cameras (Zhou et al., 2024; Zheng & Wang, 2024), LiDAR sensors (Li et al., 2023), and others (Zheng et al., 2023; 2024c;d). Recent advances in multi-sensor systems have led to the development of various approaches (Zheng et al., 2024b;a; Zhang et al., 2023a) and datasets (Zhang et al., 2023b; Brödermann et al., 2024) that extend from dual-modality fusion to full multimodal fusion, with the aim of achieving robust perception across diverse lighting and environmental conditions

throughout the day (Brödermann et al., 2023; Wei et al., 2023; Zhang et al., 2021; Man et al., 2023; Wang et al., 2022; Chen et al., 2021; Zhang et al., 2023b;a). For instance, MUSES (Brödermann et al., 2024) dataset integrates data from a frame camera, LiDAR, radar, event camera, and IMU/GNSS sensors to capture driving scenes in adverse conditions with increased uncertainty. Recently, CM-NeXt (Zhang et al., 2023b) introduced the task of fusing an arbitrary number of modalities, although this approach still relies primarily on RGB input for optimal performance. In our work, we address the challenge of *unimodal bias* in multimodal semantic segmentation by focusing on developing a robust anymodal segmentor that can maintain performance across various input combinations, rather than solely optimizing for multimodal segmentation accuracy.

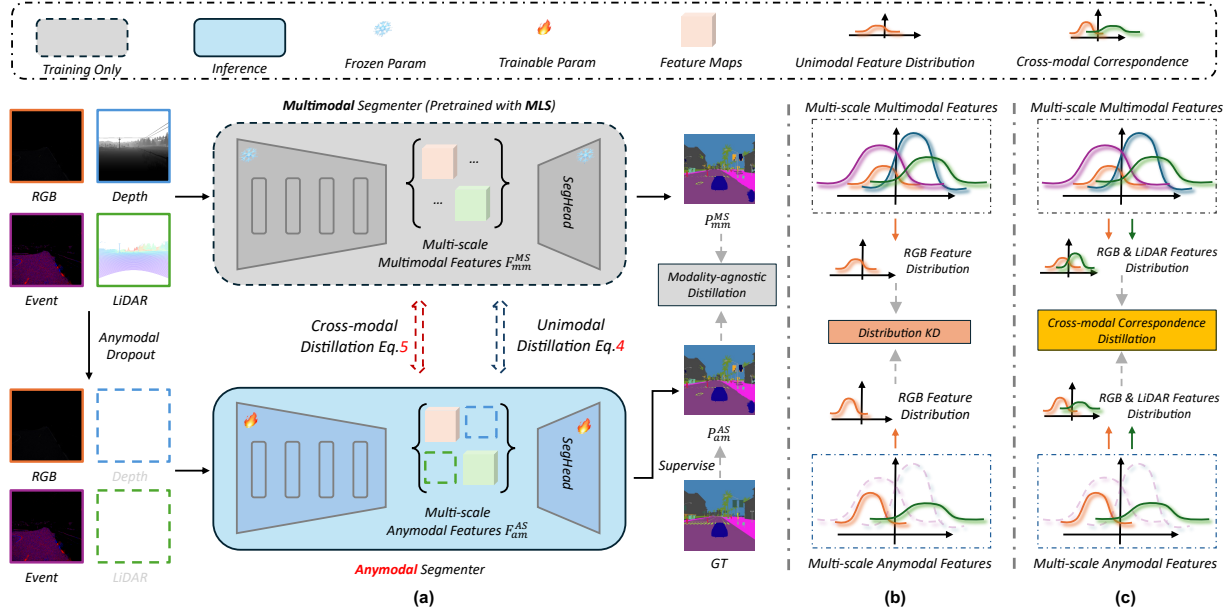
2.2. Missing Modality Robustness

In the multimodal learning community, several studies have sought to understand unimodal bias from both empirical (Kleinman et al., 2023; Peng et al., 2022) and theoretical perspectives (Huang et al., 2022). As shown by Huang *et al.* (Huang et al., 2022; Zhang et al., 2024), while multimodal learning has the potential to surpass unimodal performance, it often falls short due to modality competition: only the subset of modalities more closely aligned with the encoder’s initial parameters tends to dominate learning within the multimodal network. This phenomenon also occurs in multimodal semantic segmentation, as MAGIC (Zheng et al., 2024b) and Any2Seg (Zheng et al., 2024a) struggle when depth data is missing during inference. However, these studies are limited to relatively simple network architectures, typically using shallow networks, which constrains the applicability of their findings to real-world settings. In this work, we focus on addressing practical challenges in multi-sensor systems that are widely applicable across industrial domains, including autonomous driving and intelligent systems. We define the unimodal bias problems in multimodal semantic segmentation and propose the anymodal framework to evaluate the robustness of multimodal segmentors.

2.3. Robust Multimodal Segmentors

In practical applications, sensor failures or malfunctions often lead to incomplete multimodal data, posing significant challenges for existing segmentation frameworks, which are typically trained and evaluated with full data pairs (Liu et al., 2024). Recent research has focused on developing robust models that, although trained with complete modality sets, can accommodate the random absence of certain modalities during deployment (Liu et al., 2024; Wang et al., 2023b; Maheshwari et al., 2024; Reza et al., 2023; Chen et al., 2023; Zhao et al., 2023). Wang *et al.* (Wang et al., 2023a) proposed a method to adaptively identify crucial modalities and distill knowledge from them, enabling cross-

²<https://github.com/zhengxuJosh/AnySeg>



modal compensation for missing modalities. Liu *et. al* (Liu *et al.*, 2024) extended this idea by introducing modality-incomplete scene segmentation, addressing both system-level and sensor-level deficiencies. More recently, methods such as MAGIC (Zheng *et al.*, 2024b) and Any2Seg (Zheng *et al.*, 2024a) aim to achieve modality-agnostic segmentation by treating each modality equally and extracting shared, modality-agnostic representations. However, experimental results indicate that the fundamental issue of unimodal bias persists. For example, in the modality-incomplete evaluation of Any2Seg, performance drops significantly when depth data is absent (RD: 68.21 \rightarrow R: 39.02 with a drop of 29.19 mIoU), highlighting the ongoing challenge of unimodal bias in multimodal semantic segmentation. To address this, we propose the *first* framework for learning robust anymodal segmentors that can withstand real-world scenarios with missing modalities by distilling both multimodal and unimodal knowledge. Additionally, we introduce a parallel multimodal learning strategy as a strong baseline, further advancing robust anymodal segmentation.

3. Methodology

The overall framework is depicted in Fig. 2. It consists of two segmentors, *i.e.*, the multimodal segmentor \mathcal{F}_{ms} and anymodel segmentor \mathcal{F}_{as} , as well as two key modules, including the Unimodal and Multimodal Distillation and the Modality-agnostic Semantic Distillation modules. The multimodal segmentor \mathcal{F}_{ms} is first pre-trained with our proposed parallel multimodal learning strategy to learn a strong teacher with expertise in multimodal scenarios, its parameter is frozen during training the anymodal segmentor \mathcal{F}_{as} .

Inputs. Our framework processes multi-modal visual data from four modalities, all within the same scene. We consider RGB images $\mathbf{R} \in \mathbb{R}^{h \times w \times 3}$, depth maps $\mathbf{D} \in \mathbb{D}^{h \times w \times C^D}$, LiDAR data $\mathbf{L} \in \mathbb{L}^{h \times w \times C^P}$, and event stack images $\mathbf{E} \in \mathbb{E}^{h \times w \times C^E}$ to illustrate our method, as depicted in Fig. 2. Here, we follow the data processing as (Zhang *et al.*, 2023b), where the channel dimensions $C^D = C^P = C^E = 3$. Our framework also integrates the corresponding ground truth Y across K categories. For each training iteration, our framework takes a mini-batch $\{r, d, e, l\}$ containing samples from all the input modalities.

3.1. Parallel Multimodal Learning (PML) Strategy

Recent studies have shown that treating all input modalities equally can enhance multimodal performance in semantic segmentation (Zheng *et al.*, 2024a;b). Building on insights from MAGIC (Zheng *et al.*, 2024b), we adopt a uniform approach for handling all multimodal inputs and introduce a parallel multimodal learning strategy to train a robust teacher model for knowledge distillation. As illustrated in Fig. 3, we compute the mean across multimodal features at each block of the segmentation backbone (Xie *et al.*, 2021). This averaged output serves as the input for the segmentation head, leading to improved multimodal performance, particularly on real-world benchmarks, achieving 51.37 mIoU on MUSES. The supervised loss \mathcal{L}_{pre} for training is:

$$\mathcal{L}_{pre} = - \sum_{i=1}^N \sum_{k=1}^K y_{i,k} \log(p_{i,k}), \quad (1)$$

where $N = h \times w$ is the total number of pixels, $y_{i,k}$ is the ground truth label for class k at pixel i , and $p_{i,k}$ is the predicted probability for class k at pixel i . \mathcal{L}_{pre} encourages

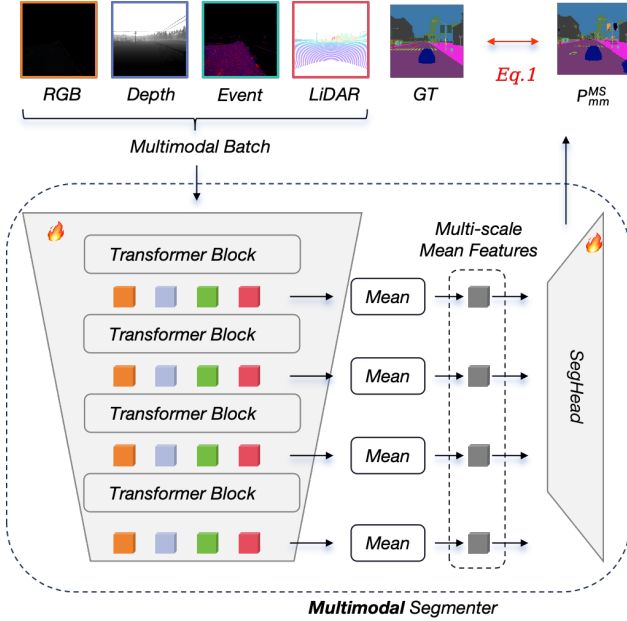


Figure 3. PML for learning a strong multimodal segmentor.

accurate predictions across all modalities and contributes to the robustness of the teacher model.

3.2. Unimodal and Multimodal Distillation

After obtaining the strong multimodal teacher \mathcal{F}_{ms} , we turn to learn efficient and robust anymodal segmentor \mathcal{F}_{as} . As depicted in Fig. 2, the input multimodal mini-batch $\{r, d, l, e\}$ is directly ingested by weight-shared encoder within the multimodal segmentor \mathcal{F}_{ms} . This process yields multi-scale features $\{f_r^i, f_d^i, f_e^i, f_l^i\}_{i=1}^4$:

$$\{f_r^i, f_d^i, f_e^i, f_l^i\}_{i=1}^4 = F_{ma}(\{r, d, l, e\}), \quad (2)$$

where i represents the multi-scale feature level, summed from 1 to 4. Meanwhile, the input multimodal mini-batch r, d, l, e undergoes random masking to generate an anymodal batch, where modality data is randomly dropped from the batch, ensuring that at least one modality is retained in each instance. The anymodal batch is then processed by the encoder of the anymodal segmentor, yielding features $g_r^i, g_{d_{i=1}}^i$ ³ for the retained modalities:

$$\{g_r^i, g_{d_{i=1}}^i\}_{i=1}^4 = \mathcal{F}_{as}(\{r, d\}). \quad (3)$$

This process ensures that the anymodal segmentor is trained on diverse input combinations, improving its robustness and adaptability to incomplete data.

Unimodal Distillation. After extracting the multi-scale features $\{f_r^i, f_d^i, f_e^i, f_l^i\}_{i=1}^4$ and $\{g_r^i, g_{d_{i=1}}^i\}_{i=1}^4$ from the multimodal segmentor (teacher model) and the anymodal segmentor (student model), respectively, we proceed with the distillation process. For the remaining multi-scale features

³For example, we illustrate the case where the event and LiDAR modalities are dropped.

$\{g_r^i, g_{d_{i=1}}^i\}_{i=1}^4$ from the anymodal segmentor \mathcal{F}_{am} , we align them with the corresponding features $\{f_r^i, f_d^i, f_e^i, f_l^i\}_{i=1}^4$ obtained from the multimodal segmentor. The unimodal knowledge distillation loss function based on KL divergency is then formulated as:

$$\mathcal{L}_{umd} = \sum_{i=1}^4 \left(\sum_{j=1}^{C_i} g_r^{i,j} \log \left(\frac{g_r^{i,j}}{f_r^{i,j}} \right) + \sum_{j=1}^{C_i} g_{d_{i=1}}^{i,j} \log \left(\frac{g_{d_{i=1}}^{i,j}}{f_d^{i,j}} \right) \right), \quad (4)$$

where C_i denotes the channel count of the i -th level features. \mathcal{L}_{umd} facilitates the transfer of knowledge within each modality, thereby enhancing the performance of the anymodal segmentor in handling single-modality data. This is demonstrated in Tab. 5, where we show the performance improvements achieved by applying unimodal distillation in the anymodal segmentation task. However, while unimodal knowledge transfer enhances single-modality performance, especially for the RGB images, it simultaneously hinders multimodal performance when different modality combinations are encountered, as also illustrated in Tab. 5.

Cross-modal Correspondence Distillation.

While unimodal knowledge distillation significantly improves segmentation performance on RGB images, as shown in Tab. 5, it also introduces unimodal bias that reduces performance on other modalities. This bias causes the model to over-rely on the RGB modality, which is easier for the model to learn, thereby limiting its generalization capacity across diverse input types. Consequently, unimodal knowledge transfer, while beneficial for single-modality performance, negatively impacts multimodal performance in mixed-modality scenarios. This is evident in Tab. 5, where performance decreases for modalities such as Event (-3.74% ↓) and LiDAR (-2.91% ↓).

To address this, we leverage cross-modal correspondences between “easy-to-learn” and “hard-to-learn” modalities to achieve a more balanced performance. By distilling these cross-modal relationships from the teacher model to the student model—referred to as the “anymodal” segmentor—we effectively mitigate unimodal bias and enhance performance across all modalities.

The distillation of cross-modal knowledge between student features $\{g_r^i, g_{d_{i=1}}^i\}_{i=1}^4$ and teacher features $\{f_r^i, f_d^i, f_e^i, f_l^i\}_{i=1}^4$ is achieved through:

$$\mathcal{L}_{cmd} = \sum_{i=1}^4 \sum_{j=1}^{C_i} \mathcal{S} \left(g_d^{i,j}, g_r^{i,j} \right) \log \left(\frac{\mathcal{S} \left(g_d^{i,j}, g_r^{i,j} \right)}{\mathcal{S} \left(f_d^{i,j}, f_r^{i,j} \right)} \right), \quad (5)$$

where $\mathcal{S}(x, y) = \frac{x \cdot y}{\|x\| \|y\|}$ denotes cosine similarity between feature vectors x and y . This formulation aligns cross-modal representations by minimizing the discrepancy between teacher and student model similarities across modalities.

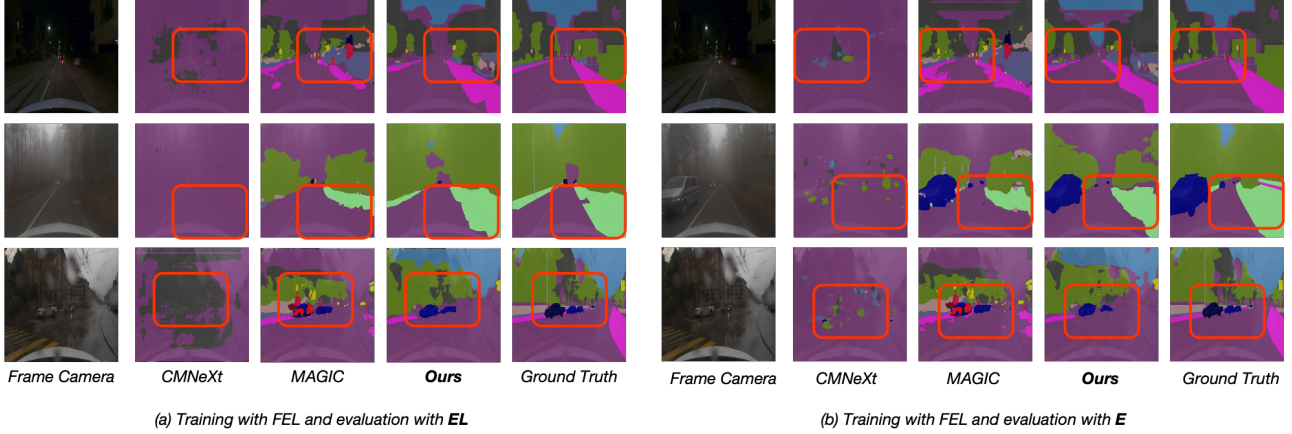


Figure 4. Qualitative comparison between CMNeXt (Zhang et al., 2023b), MAGIC (Zheng et al., 2024b) and ours on MUSES.

Table 1. Results of anymodal semantic segmentation validation with three modalities on real-world benchmark MUSES dataset using SegFormer-B0 as backbone model.

Method	Pub.	Training	Anymodal Evaluation							Mean
			F	E	L	FE	FL	EL	FEL	
CMX (Zhang et al., 2023a)	T-ITS 2023	FEL	2.52	2.35	3.01	41.15	41.25	2.56	42.27	19.30
CMNeXt (Zhang et al., 2023b)	CVPR 2023		3.50	2.77	2.64	6.63	10.28	3.14	46.66	10.80
MAGIC (Zheng et al., 2024b)	ECCV 2024		43.22	2.68	<u>22.95</u>	43.51	49.05	<u>22.98</u>	49.02	33.34
Any2Seg (Zheng et al., 2024a)	ECCV 2024		<u>44.40</u>	<u>3.17</u>	22.33	44.51	<u>49.96</u>	22.63	<u>50.00</u>	<u>33.86</u>
Ours	-		46.01	19.57	32.13	46.29	51.25	35.21	51.14	40.23
<i>w.r.t</i> SoTA	-	-	+1.61	+16.40	+9.80	+1.78	+1.29	+12.58	+1.14	+6.37

After applying cross-modal correspondence distillation, the inherent unimodal bias in this task—as well as the bias introduced by unimodal knowledge distillation—are largely mitigated, as shown in Tab. 5.

3.3. Modality-agnostic Distillation

After addressing the unimodal bias problem in the representation spaces, we also focus on transferring task-related semantic information at the prediction level for further utilization of the pre-trained knowledge in the teacher model. Specifically, the segmentation maps predicted by the multimodal teacher P_{mm} are used as supervision signals for the predictions of the anymodal student segmentor P_{am} . The modality-agnostic distillation loss is formulated as:

$$\mathcal{L}_{mad} = \frac{1}{N} \sum_{i=1}^N \sum_{k=1}^K P_{am}^{i,k} \log \left(\frac{P_{am}^{i,k}}{P_{mm}^{i,k}} \right). \quad (6)$$

Additionally, there is also a supervised loss imposed between the P_{am} and the GT:

$$\mathcal{L}_{sup} = -\frac{1}{N} \sum_{i=1}^N \sum_{k=1}^K y_k^i \log (P_{am}^{i,k}). \quad (7)$$

The total loss for training the anymodal student segmentor combines the modality-agnostic distillation loss and the

supervised loss as follows:

$$\mathcal{L}_{total} = \mathcal{L}_{sup} + \lambda \mathcal{L}_{mad} + \alpha \mathcal{L}_{umd} + \beta \mathcal{L}_{cmd}, \quad (8)$$

where λ_{mad} and λ_{sup} are weighting factors that balance the contributions of the two loss terms.

4. Experiments

4.1. Experimental Setup

Datasets. We evaluate our proposed method on both synthetic and real-world multi-sensor datasets. The MUSES dataset (Brödermann et al., 2024) consists of driving sequences recorded in Switzerland, specifically designed to tackle challenges posed by adverse visual conditions. It features multi-sensor readings, including a high-resolution frame camera, an event camera, and MEMS LiDAR, providing complementary modalities to enhance annotation quality and support robust multimodal semantic segmentation. Each sequence is meticulously annotated with high-quality 2D panoptic labels, ensuring accurate ground truth for comprehensive benchmarking. The DELIVER dataset (Zhang et al., 2023b) is a diverse multimodal dataset comprising RGB, depth, LiDAR, and event data across 25 semantic categories. It covers various environmental conditions and includes scenarios with sensor failures, enabling thorough evaluations under challenging situations. For our experiments, we

Table 2. Results of anymodal semantic segmentation validation with three modalities on synthetic benchmark DELIVER dataset using SegFormer-B0 as backbone model.

Method	Anymodal Evaluation															Mean
	R	D	E	L	RD	RE	RL	DE	DL	EL	RDE	RDL	REL	DEL	RDEL	
CMNeXt (Zhang et al., 2023b)	0.86	0.49	0.66	0.37	47.06	9.97	13.75	2.63	1.73	2.85	59.03	59.18	14.73	59.18	39.07	20.77
MAGIC (Zheng et al., 2024b)	32.60	55.06	0.52	0.39	63.32	33.02	33.12	55.16	55.17	0.26	63.37	63.36	33.32	55.26	63.40	40.49
Ours	47.11	<u>52.17</u>	17.33	19.01	<u>60.37</u>	47.49	48.13	<u>52.82</u>	<u>52.29</u>	21.47	<u>60.16</u>	<u>60.60</u>	47.98	52.44	<u>60.26</u>	46.64
w.r.t SoTA	+14.51	-2.89	+16.81	+18.62	-2.95	+14.47	+15.01	-2.34	-2.88	+21.21	-3.21	-2.76	+14.66	-2.82	-3.14	+6.15

Table 3. Ablation study of different loss function combinations in our framework on MUSES dataset (Brödermann et al., 2024).

Loss Combination	F	$\Delta \uparrow$	E	$\Delta \uparrow$	L	$\Delta \uparrow$	FE	$\Delta \uparrow$	FL	$\Delta \uparrow$	EL	$\Delta \uparrow$	FEL	$\Delta \uparrow$	Mean	$\Delta \uparrow$
\mathcal{L}_{sup}	43.69	-	22.35	-	32.14	-	44.58	-	48.53	-	35.40	-	48.35	-	39.29	-
$\mathcal{L}_{sup} + \lambda\mathcal{L}_{mad}$	43.71	+0.02	23.00	+0.65	34.70	+2.56	44.18	-0.40	49.13	+0.60	37.23	+1.83	48.79	+0.44	40.11	+0.82
$\mathcal{L}_{sup} + \lambda\mathcal{L}_{mad} + \alpha\mathcal{L}_{umd}$	45.82	+2.13	19.26	-3.09	31.79	-0.35	45.88	+1.30	51.11	+2.58	33.56	-1.84	50.60	+0.43	39.72	+0.43
$\mathcal{L}_{sup} + \lambda\mathcal{L}_{mad} + \alpha\mathcal{L}_{umd} + \beta\mathcal{L}_{cmd}$	46.01	+2.32	19.57	-2.78	32.13	-0.01	46.29	+1.71	51.25	+2.72	35.21	-0.21	51.14	+2.79	40.23	+0.94

follow the official data processing and split protocols.

Implementation Details. All experiments on the MUSES dataset were conducted on 8 NVIDIA 3090 GPUs, while experiments on the DELIVER dataset utilized 4 NVIDIA A100 GPUs. The initial learning rate was set to 6×10^{-5} and adjusted using a polynomial decay strategy with a power of 0.9 over 200 epochs. Additionally, a 10-epoch warm-up phase was applied at 10% of the initial learning rate to stabilize training. The AdamW optimizer was employed, and the effective batch size for both datasets was set to 16. Input modality data was cropped to 1024×1024 resolution for consistency across benchmarks.

4.2. Results

As presented in Tab. 1, the proposed method achieves the highest mIoU of **40.23**, outperforming all state-of-the-art (SoTA) methods. CMX (Zhang et al., 2023a) and CMNeXt (Zhang et al., 2023b) show weaker performance (mIoU: 19.30 and 10.80, respectively), struggling with individual modalities due to their reliance on RGB. Similarly, MAGIC (Zheng et al., 2024b) and Any2Seg (Zheng et al., 2024a) rely heavily on depth data, resulting in significant performance drops when this modality is unavailable, revealing their unimodal bias. In contrast, our method demonstrates superior performance across all metrics, effectively mitigating unimodal bias. It achieves strong results on individual modalities—RGB (46.01), Event (19.57), and LiDAR (32.13)—and excels in paired modalities, such as FE (46.29), FL (51.25), and EL (35.21), as well as combined modalities like FEL (51.14), showcasing its cross-modal learning capability. Notably, our method achieves significant gains in challenging scenarios, such as Event data (+16.40) and paired modalities involving LiDAR (e.g., FL: +12.58), highlighting its ability to leverage multimodal data and handle complex interactions. Qualitative results are shown in Fig. 4. These results demonstrate the effectiveness in achieving robust segmentation of the proposed framework.

Tab. 2 presents the results on the synthetic benchmark DELIVER using SegFormer-B0 as the backbone. Our method achieves the highest mIoU of **46.64**, representing an improvement of **+6.15** over MAGIC (Zheng et al., 2024b), the previous SoTA. In individual modalities, our method achieves mIoUs of 47.11 (R), 52.17 (D), and 19.01 (L), with improvements of +14.51 (R) and +18.62 (L) compared to MAGIC. Notably, the significant gains in Event (+16.81) and LiDAR (+18.62) underscore the method’s robustness against unimodal bias. For paired modality combinations, our approach also shows strong performance. The RD, RE, and RL combinations achieve mIoUs of 60.37, 47.49, and 48.13, with notable gains of +14.47 (RE) and +15.01 (RL) over MAGIC. These results highlight the effectiveness of the model in capturing cross-modal relationships while mitigating unimodal limitations. Overall, these results validate the superiority of our method in both individual and multimodal segmentation tasks, demonstrating its ability to handle diverse data modalities and achieve robust performance.

5. Ablation Study

5.1. Effectiveness of Loss Functions

Tab. 3 shows results of different loss function combinations on the MUSES dataset (Brödermann et al., 2024). The baseline using only the supervised loss (\mathcal{L}_{sup}) achieves a mean mIoU of 39.29. Adding the modality-adaptive loss ($\lambda\mathcal{L}_{mad}$) improves performance, with gains in paired and combined modalities. Adding the unimodal-distillation loss ($\alpha\mathcal{L}_{umd}$) to $\mathcal{L}_{sup} + \lambda\mathcal{L}_{mad}$ results in more significant gains. Notable improvements include RGB (F: +2.13), FE (+1.30), and FL (+2.58), highlighting the value of leveraging unimodal features. The full loss combination, incorporating the cross-modal distillation loss ($\beta\mathcal{L}_{cmd}$), achieves the highest mean mIoU of 40.23, with consistent improvements across all modalities. Paired modalities FL (+2.72) and FEL (+2.79) show the largest gains, while Event (E) improves slightly (+0.43). These results demonstrate the method’s robustness

Table 4. Ablation study on the effect of different parameters for L_{mad} in our framework on MUSES dataset (Brödermann et al., 2024).

λ	F	$\Delta \uparrow$	E	$\Delta \uparrow$	L	$\Delta \uparrow$	FE	$\Delta \uparrow$	FL	$\Delta \uparrow$	EL	$\Delta \uparrow$	FEL	$\Delta \uparrow$	Mean	$\Delta \uparrow$
1	43.97	-	22.33	-	31.90	-	44.82	-	48.61	-	35.14	-	48.33	-	39.30	-
10	43.84	-0.13	23.21	+0.88	32.71	+0.81	44.08	-0.74	49.16	0.55	34.97	-0.17	48.08	-0.25	39.44	+0.14
20	44.08	+0.11	22.76	+0.43	32.35	+0.45	44.37	-0.45	49.33	+0.72	34.73	-0.41	48.79	+0.46	39.49	+0.19
50	43.71	-0.26	23.00	+0.67	34.70	+2.80	44.18	-0.64	49.13	+0.52	37.23	+2.09	48.79	+0.46	40.11	+0.81
60	44.02	+0.05	22.74	+0.41	33.82	+1.92	44.29	-0.53	49.36	+0.75	36.69	+1.55	48.54	+0.21	39.92	+0.62
80	43.84	-0.13	22.86	+0.53	33.78	+1.88	44.25	-0.57	49.43	+0.82	36.57	+1.43	48.72	+0.39	39.92	+0.62
100	43.75	-0.22	22.87	+0.54	34.00	+2.10	44.17	-0.65	49.36	+0.75	36.60	+1.46	48.64	+0.31	39.91	+0.61

Table 5. Ablation study on the effect of different parameters for L_{umd} in our framework on MUSES dataset (Brödermann et al., 2024).

α	F	$\Delta \uparrow$	E	$\Delta \uparrow$	L	$\Delta \uparrow$	FE	$\Delta \uparrow$	FL	$\Delta \uparrow$	EL	$\Delta \uparrow$	FEL	$\Delta \uparrow$	Mean	$\Delta \uparrow$
w/o	43.71	-	23.00	-	34.70	-	44.18	-	49.13	-	37.23	-	48.79	-	40.11	-
1	44.54	+0.83	22.02	-0.98	31.67	-3.03	44.66	+0.48	49.55	+0.42	33.93	-3.30	48.89	+0.10	39.32	-0.79
3	45.38	+1.67	20.64	-2.36	31.37	-3.33	45.43	+1.25	50.53	+1.40	33.65	-3.58	49.93	+1.14	39.56	-0.55
5	45.82	+2.11	19.26	-3.74	31.79	-2.91	45.88	+1.70	51.11	+1.98	33.56	-3.67	50.60	+1.81	39.72	-0.39
7	46.09	+2.38	17.84	-5.16	31.81	-2.89	46.18	+2.00	51.36	+2.23	33.43	-3.80	51.01	+2.22	39.67	-0.44
10	46.17	+2.46	15.74	-7.26	31.95	-2.75	46.37	+2.19	51.17	+2.04	33.26	-3.97	51.08	+2.29	39.39	-0.72

in handling complex multimodal interactions. Overall, each loss component plays a critical role in improving anymodal segmentation, with the full combination proving most effective in leveraging multimodal data for real-world scenarios.

5.2. Ablation on Hyper-Parameter Selection

We analyze the impact of hyper-parameters for \mathcal{L}_{mad} , \mathcal{L}_{umd} , and \mathcal{L}_{cmd} in our framework. The results in Tab. 4, Tab. 5, and Tab. 6 highlight how these parameters influence performance. Tab. 4 evaluates the effect of varying λ . The baseline ($\lambda = 1$) achieves a mean mIoU of 39.30. Increasing λ improves performance, peaking at $\lambda = 50$ with a mean mIoU of **40.11** (+0.81). Significant gains are observed in LiDAR (L: +2.80) and Event-LiDAR (EL: +2.09), demonstrating \mathcal{L}_{mad} 's effectiveness in enhancing underrepresented modalities. Further increases ($\lambda > 50$) yield diminishing returns, indicating a trade-off between distillation strength and stability. Tab. 5 examines the effect of varying α . Without \mathcal{L}_{umd} (w/o), the mean mIoU is 40.11. The highest performance is achieved with $\alpha = 2$, yielding a mean mIoU of **40.22** (+0.11), with notable gains in RGB (F: +2.11), FL (+2.00), and FEL (+2.29). Larger α values ($\alpha > 5$) reduce performance, highlighting the need to balance unimodal and cross-modal contributions.

Tab. 6 studies \mathcal{L}_{cmd} with varying β while keeping \mathcal{L}_{umd} fixed. The baseline ($\beta = 0$) achieves a mean mIoU of 39.72. Adding \mathcal{L}_{cmd} with $\beta = 5$ improves the mean mIoU to **40.21** (+0.49), with strong gains in Event-LiDAR (EL: +2.04) and FL (+1.62). Larger β values ($\beta > 10$) degrade performance, suggesting overemphasis on cross-modal distillation can overshadow unimodal contributions. Optimal values of λ , α , and β are crucial for maximizing each loss's benefits. While \mathcal{L}_{mad} addresses unimodal biases, \mathcal{L}_{umd} and \mathcal{L}_{cmd} enhance

both unimodal and cross-modal interactions, enabling robust anymodal segmentation.

5.3. Rationality of Unimodal Distillation

The effectiveness of \mathcal{L}_{umd} is demonstrated in Tab. 5. Adding \mathcal{L}_{umd} with $\alpha = 1$ improves single-modality performance, particularly for RGB (F : +0.83) and paired modalities such as FL (+0.42). The best performance for single-modality tasks is observed at $\alpha = 10$, where the mean mIoU for RGB increases to **46.17** (+2.46), and FL achieves **51.17** (+2.19). Obviously, \mathcal{L}_{umd} effectively improves single-modality segmentation performance by facilitating knowledge transfer within each modality. However, the results also highlight a trade-off: while unimodal distillation enhances performance for individual modalities, it may compromise the model's ability to handle complex multimodal combinations. Careful tuning of α is therefore critical to achieving a balance between single-modality and multimodal segmentation performance.

Rationality of Cross-modal Distillation. Unimodal knowledge distillation improves segmentation performance on RGB images but introduces unimodal bias, reducing performance on other modalities. This bias arises as the model over-relies on RGB, which is easier to learn, limiting its generalization across diverse inputs. As shown in Tab. 5, performance on Event (-3.74%) and LiDAR (-2.91%) modalities declines significantly. While unimodal knowledge transfer enhances single-modality performance, it negatively impacts multimodal performance in mixed-modality scenarios. Cross-modal correspondence distillation mitigates this bias by aligning representations across modalities, improving segmentation performance on diverse inputs. It balances the trade-off between single-modality and multimodal perfor-

Table 6. Ablation study on the effect of different parameters for add L_{cmd} with L_{umd} on MUSES dataset (Brödermann et al., 2024). w/o means the framework is only trained with $L_{mad} + L_{umd}$.

β	F	$\Delta \uparrow$	E	$\Delta \uparrow$	L	$\Delta \uparrow$	FE	$\Delta \uparrow$	FL	$\Delta \uparrow$	EL	$\Delta \uparrow$	FEL	$\Delta \uparrow$	Mean	$\Delta \uparrow$
w/o	45.82	-	19.26	-	31.79	-	45.88	-	51.11	-	33.56	-	50.60	-	39.72	-
1	45.93	+0.11	18.76	-0.50	31.84	+0.05	45.96	+0.08	51.22	+0.11	33.49	-0.07	50.82	+0.22	39.72	0.00
3	46.04	+0.22	17.74	-1.52	31.42	-0.37	46.08	+0.20	51.27	+0.16	33.46	-0.10	50.99	+0.39	39.57	-0.15
5	46.19	+0.37	17.27	-1.99	31.03	-0.76	46.27	+0.39	51.34	+0.33	33.40	-0.16	51.05	+0.45	39.51	-0.21
7	46.21	+0.39	17.40	-1.86	31.06	-0.73	46.37	+0.49	51.29	+0.18	33.79	+0.23	51.12	-0.12	39.60	-0.12
10	46.01	+0.19	19.57	+0.31	32.13	+0.34	46.29	+0.41	51.25	+0.14	35.21	+1.65	51.14	+0.54	40.23	+0.51
13	46.57	+0.75	18.24	-1.02	30.88	-0.91	46.74	+0.86	51.09	-0.02	33.88	+0.32	50.76	+0.16	39.74	+0.02
15	46.03	+0.21	14.10	-8.90	31.12	-3.58	45.99	+1.81	50.97	+1.84	31.42	-5.81	50.49	-0.11	38.59	-1.13
20	45.95	+0.13	15.19	-7.81	30.61	-4.09	45.80	+1.62	51.19	+2.06	30.55	-6.68	50.41	+1.62	38.53	-1.58

Table 7. Discussion study on the effect of performing knowledge distillation with fused features on MUSES dataset (Brödermann et al., 2024). w/o means the framework is only trained with $L_{mad} + L_{umd} + L_{cmd}$.

λ	F	$\Delta \uparrow$	E	$\Delta \uparrow$	L	$\Delta \uparrow$	FE	$\Delta \uparrow$	FL	$\Delta \uparrow$	EL	$\Delta \uparrow$	FEL	$\Delta \uparrow$	Mean	$\Delta \uparrow$
w/o	46.01	-	19.57	-	32.13	-	46.29	-	51.25	-	35.21	-	51.14	-	40.23	-
1	46.32	+0.31	17.99	-1.58	31.38	-0.75	46.80	+0.51	51.01	-0.24	33.92	-1.29	50.95	-0.19	39.77	-0.46
3	46.34	+0.33	17.27	-2.30	31.36	-0.77	46.81	+0.52	51.20	-0.05	33.87	-1.34	51.13	-0.01	39.71	-0.52
5	46.34	+0.33	16.72	-2.85	31.41	-0.72	46.79	+0.50	51.23	-0.02	33.88	-1.33	51.17	+0.03	39.65	-0.58
7	46.28	+0.27	18.01	-1.56	31.47	-0.66	46.76	+0.47	51.05	-0.20	33.99	-1.22	50.97	-0.17	39.79	-0.44
10	46.10	+0.09	15.61	-3.96	31.39	-0.74	46.55	+0.26	51.23	-0.02	33.59	-1.62	51.14	+0.00	39.37	-0.86

mance, emphasizing the need to carefully tune β for optimal results. However, larger β values ($\beta > 13$) degrade performance, particularly on Event (-8.90%) and LiDAR (-3.58%), suggesting that overemphasizing cross-modal distillation can overshadow individual modality learning, leading to performance trade-offs.

5.4. Why not KD between Fused Features?

To explore the possibility of transferring knowledge between fused features from teacher to student models, we conduct experiments on the MUSES dataset, leveraging the fusion method described in (Zheng et al., 2024b). The results are summarized in Tab. 7. It is evident that applying knowledge distillation (KD) directly on fused features causes a notable performance drop across most metrics. For instance, compared to the baseline without KD on fused features (w/o), which achieves a mean mIoU of 40.23, all settings with KD exhibit reduced performance. At $\lambda = 1$, the mean mIoU drops to 39.77 (-0.46), while higher λ values exacerbate the decline, with $\lambda = 10$ resulting in a mean mIoU of 39.37 (-0.86). These results highlight the inefficacy of such distillation methods. Examining individual modalities further reveals this trend. For the Event (E) and LiDAR (L) modalities, performance consistently degrades as λ increases, with Event mIoU decreasing by up to -3.96 at $\lambda = 10$. Paired and fused modalities also show minimal improvement or slight degradation, such as FEL achieving a marginal gain of

+0.03 at $\lambda = 5$ but regressing at $\lambda = 10$. The results suggest that directly applying knowledge distillation between fused features fails to effectively guide the student model. Instead of transferring meaningful knowledge, the fused features introduce noise and misalignment, limiting their utility in this context. This reinforces the importance of designing specialized mechanisms for knowledge distillation, targeting individual or structured features rather than indiscriminately fused representations.

6. Conclusion

In this paper, we addressed the challenge of unimodal bias in multimodal semantic segmentation, where reliance on specific modalities leads to performance drops when modalities are missing. We proposed the first framework for any-modal segmentation using unimodal and cross-modal distillation. A PML strategy ensures a strong teacher model, while multiscale distillation transfers feature-level knowledge. By distilling unimodal distributions with cross-modal correspondences, we reduce modality dependency. Additionally, modality-agnostic semantic distillation enables robust prediction-level knowledge transfer. Experiments on synthetic and real multi-sensor benchmarks validate the superior performance of our framework. Furthermore, our discussion on fused feature distillation highlights the need for specialized mechanisms targeting individual or structured features rather than indiscriminate fusion.

References

- Brödermann, T., Bruggemann, D., Sakaridis, C., Ta, K., Liagouris, O., Corkill, J., and Van Gool, L. Muses: The multi-sensor semantic perception dataset for driving under uncertainty. In *Proceedings of the European Conference on Computer Vision*, 2024.
- Broedermann, T., Sakaridis, C., Dai, D., and Van Gool, L. Hrfuser: A multi-resolution sensor fusion architecture for 2d object detection. In *IEEE International Conference on Intelligent Transportation Systems*, pp. 4159–4166, 2023.
- Chen, L.-Z., Lin, Z., Wang, Z., Yang, Y.-L., and Cheng, M.-M. Spatial information guided convolution for real-time rgbd semantic segmentation. *IEEE Transactions on Image Processing*, 30:2313–2324, 2021.
- Chen, M., Yao, J., Xing, L., Wang, Y., Zhang, Y., and Wang, Y. Redundancy-adaptive multimodal learning for imperfect data. *arXiv preprint arXiv:2310.14496*, 2023.
- Huang, Y., Lin, J., Zhou, C., Yang, H., and Huang, L. Modality competition: What makes joint training of multi-modal network fail in deep learning? (provably). In *International Conference on Machine Learning*, pp. 9226–9259, 2022.
- Kleinman, M., Achille, A., and Soatto, S. Critical learning periods for multisensory integration in deep networks. In *Proceedings of the IEEE/CVF Conference on Computer Vision and Pattern Recognition*, pp. 24296–24305, 2023.
- Li, J., Dai, H., Han, H., and Ding, Y. Mseg3d: Multi-modal 3d semantic segmentation for autonomous driving. In *Proceedings of the IEEE/CVF Conference on Computer Vision and Pattern Recognition*, pp. 21694–21704, 2023.
- Liu, R., Zhang, J., Peng, K., Chen, Y., Cao, K., Zheng, J., Sarfraz, M. S., Yang, K., and Stiefelhagen, R. Fourier prompt tuning for modality-incomplete scene segmentation. In *IEEE Intelligent Vehicles Symposium*, pp. 961–968, 2024.
- Maheshwari, H., Liu, Y.-C., and Kira, Z. Missing modality robustness in semi-supervised multi-modal semantic segmentation. In *Proceedings of the IEEE/CVF Winter Conference on Applications of Computer Vision*, pp. 1020–1030, 2024.
- Man, Y., Gui, L.-Y., and Wang, Y.-X. Bev-guided multi-modality fusion for driving perception. In *Proceedings of the IEEE/CVF Conference on Computer Vision and Pattern Recognition*, pp. 21960–21969, 2023.
- Peng, X., Wei, Y., Deng, A., Wang, D., and Hu, D. Balanced multimodal learning via on-the-fly gradient modulation. In *Proceedings of the IEEE/CVF Conference on Computer Vision and Pattern Recognition*, pp. 8238–8247, 2022.
- Reza, M. K., Prater-Bennette, A., and Asif, M. S. Robust multimodal learning with missing modalities via parameter-efficient adaptation. *arXiv preprint arXiv:2310.03986*, 2023.
- Wang, H., Ma, C., Zhang, J., Zhang, Y., Avery, J., Hull, L., and Carneiro, G. Learnable cross-modal knowledge distillation for multi-modal learning with missing modality. In *International Conference on Medical Image Computing and Computer-Assisted Intervention*, pp. 216–226, 2023a.
- Wang, Y., Chen, X., Cao, L., Huang, W., Sun, F., and Wang, Y. Multimodal token fusion for vision transformers. In *Proceedings of the IEEE/CVF Conference on Computer Vision and Pattern Recognition*, pp. 12186–12195, 2022.
- Wang, Y., Mao, Q., Zhu, H., Deng, J., Zhang, Y., Ji, J., Li, H., and Zhang, Y. Multi-modal 3d object detection in autonomous driving: a survey. *International Journal of Computer Vision*, pp. 1–31, 2023b.
- Wei, S., Luo, C., and Luo, Y. Mmanet: Margin-aware distillation and modality-aware regularization for incomplete multimodal learning. In *Proceedings of the IEEE/CVF Conference on Computer Vision and Pattern Recognition*, pp. 20039–20049, 2023.
- Xie, E., Wang, W., Yu, Z., Anandkumar, A., Alvarez, J. M., and Luo, P. Segformer: Simple and efficient design for semantic segmentation with transformers. *Advances in neural information processing systems*, 34:12077–12090, 2021.
- Zhang, J., Liu, H., Yang, K., Hu, X., Liu, R., and Stiefelhagen, R. Cmx: Cross-modal fusion for rgb-x semantic segmentation with transformers. *IEEE Transactions on intelligent transportation systems*, 2023a.
- Zhang, J., Liu, R., Shi, H., Yang, K., Reiß, S., Peng, K., Fu, H., Wang, K., and Stiefelhagen, R. Delivering arbitrary-modal semantic segmentation. In *Proceedings of the IEEE/CVF Conference on Computer Vision and Pattern Recognition*, pp. 1136–1147, 2023b.
- Zhang, Q., Zhao, S., Luo, Y., Zhang, D., Huang, N., and Han, J. Abmdrnet: Adaptive-weighted bi-directional modality difference reduction network for rgb-t semantic segmentation. In *Proceedings of the IEEE/CVF Conference on Computer Vision and Pattern Recognition*, pp. 2633–2642, 2021.
- Zhang, Y., Latham, P. E., and Saxe, A. M. Understanding unimodal bias in multimodal deep linear networks. In *International Conference on Machine Learning*, 2024.

- Zhao, Z., Palani, H., Liu, T., Evans, L., and Toner, R. Multi-modality guidance network for missing modality inference. *arXiv preprint arXiv:2309.03452*, 2023.
- Zheng, X. and Wang, L. Eventdance: Unsupervised source-free cross-modal adaptation for event-based object recognition. In *Proceedings of the IEEE/CVF Conference on Computer Vision and Pattern Recognition*, pp. 17448–17458, 2024.
- Zheng, X., Zhu, J., Liu, Y., Cao, Z., Fu, C., and Wang, L. Both style and distortion matter: Dual-path unsupervised domain adaptation for panoramic semantic segmentation. In *Proceedings of the IEEE/CVF Conference on Computer Vision and Pattern Recognition*, pp. 1285–1295, 2023.
- Zheng, X., Lyu, Y., and Wang, L. Learning modality-agnostic representation for semantic segmentation from any modalities. In *Proceedings of the European Conference on Computer Vision*, 2024a.
- Zheng, X., Lyu, Y., Zhou, J., and Wang, L. Centering the value of every modality: Towards efficient and resilient modality-agnostic semantic segmentation. In *Proceedings of the European Conference on Computer Vision*, 2024b.
- Zheng, X., Zhou, P., Vasilakos, A. V., and Wang, L. Semantics distortion and style matter: Towards source-free uda for panoramic segmentation. In *Proceedings of the IEEE/CVF Conference on Computer Vision and Pattern Recognition*, pp. 27885–27895, 2024c.
- Zheng, X., Zhou, P. Y., Vasilakos, A. V., and Wang, L. 360sfuda++: Towards source-free uda for panoramic segmentation by learning reliable category prototypes. *IEEE Transactions on Pattern Analysis and Machine Intelligence*, 2024d.
- Zhou, J., Zheng, X., Lyu, Y., and Wang, L. Eventbind: Learning a unified representation to bind them all for event-based open-world understanding. In *Proceedings of the European Conference on Computer Vision*, 2024.